



This open access document is posted as a preprint in the Beilstein Archives at <https://doi.org/10.3762/bxiv.2021.62.v1> and is considered to be an early communication for feedback before peer review. Before citing this document, please check if a final, peer-reviewed version has been published.

This document is not formatted, has not undergone copyediting or typesetting, and may contain errors, unsubstantiated scientific claims or preliminary data.

**Preprint Title** Host-guest interaction and properties of cucurbit[8]uril with chloramphenicol

**Authors** Lin Zhang, Jun Zheng, Guangyan Luo, Xiaoyue Li, Yunqian Zhang, Zhu Tao and Qianjun Zhang

**Publication Date** 30 Aug 2021

**Article Type** Full Research Paper

**Supporting Information File 1** Support Information.docx; 26.6 KB

**ORCID® IDs** Qianjun Zhang - <https://orcid.org/0000-0002-0131-5181>

License and Terms: This document is copyright 2021 the Author(s); licensee Beilstein-Institut.

This is an open access work under the terms of the Creative Commons Attribution License (<https://creativecommons.org/licenses/by/4.0>). Please note that the reuse, redistribution and reproduction in particular requires that the author(s) and source are credited and that individual graphics may be subject to special legal provisions.

The license is subject to the Beilstein Archives terms and conditions: <https://www.beilstein-archives.org/xiv/terms>.

The definitive version of this work can be found at <https://doi.org/10.3762/bxiv.2021.62.v1>

# Host-guest interaction and properties of cucurbit[8]uril with chloramphenicol

Lin Zhang, Jun Zheng, Guangyan Luo, XiaoYue Li, Yunqian Zhang, Zhu Tao and Qianjun Zhang\*

Key Laboratory of Macrocyclic and Supramolecular Chemistry of Guizhou Province, Guizhou University, Guiyang 550025, China.

Email: Qianjun Zhang\* - qjzhang@gzu.edu.cn

\* Corresponding author

The interaction between cucurbit[8]uril (Q[8]) and chloramphenicol (CPE) was investigated using single-crystal X-ray diffraction, spectroscopy, isothermal titration calorimetry (ITC) and UV-Vis, NMR and IR spectroscopy. The effects of Q[8] on the stability, in vitro release performance and antibacterial activity of CPE were also studied. The results showed that CPE and Q[8] formed a 1:1 inclusion complex (CPE@Q[8]) with an inclusion constant of  $5.4736 \times 10^5$  L/mol. The intervention of Q[8] did not affect the stability of CPE, but obviously reduced the release rate of CPE in artificial gastric and intestinal juice; Q[8] has a slow-release effect on CPE. The antibacterial results showed that the minimum inhibitory concentration (MIC) of CPE and CPE@Q[8] toward *Escherichia coli* (*E. coli*) was  $1.5 \times 10^{-3}$  and  $1.0 \times 10^{-3}$  mol/L, respectively, and toward *Staphylococcus aureus* (SA), the MIC was  $2.0 \times 10^{-3}$  mol/L for both CPE and CPE@Q[8]. Therefore, Q[8] enhanced the inhibitory activity of CPE against *E. coli*.

**Keywords:** Chloramphenicol, cucurbit[8]uril, host-guest interaction, stability, in vitro cumulative release, antibacterial activity.

## Introduction

Chloramphenicol (CPE, Fig. 1A) is a broad-spectrum antibiotic resulting from the metabolism of chorismic acid in *Streptomyces venezuelae*,<sup>[1]</sup> which has a certain inhibitory effect on many Gram-positive and negative cocci bacteria, as well as anaerobic bacteria,<sup>[2]</sup> and is used for the treatment of typhoid, meningitis, chlamydia,

eye infections, purulent wounds and other diseases.<sup>[3]</sup> Chloramphenicol is slightly soluble in water and has a bitter taste. Upon forming an inclusion complex with cyclodextrin, the solubility and bitter taste of CPE can be improved.<sup>[4,5]</sup> Bayrakci et al.<sup>[6]</sup> reported that the inclusion complex of cyclodextrin and chloramphenicol loaded silver nanoparticles possessed stronger antibacterial properties than CPE alone.

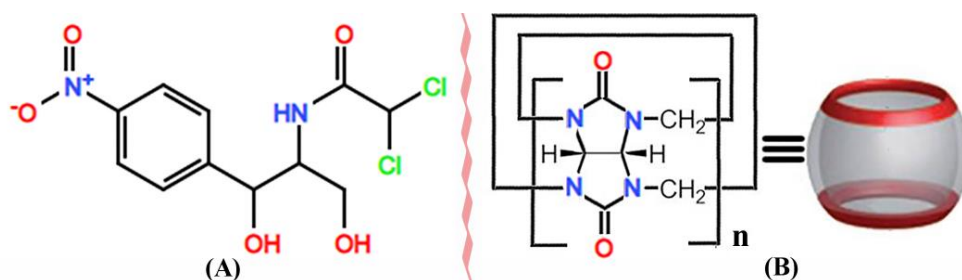


Fig.1 The structures of chloramphenicol (A) and Cucurbit[n]urils (B)

As a new type of supramolecular host compound, cucurbit[n]urils<sup>[7–18]</sup> (Q[n]s, Fig. 1B) form via the polymerization of multiple glycoside units. The ports on both sides of these compounds are surrounded by carbonyl oxygen atoms, which form a hydrophobic cavity and two hydrophilic ports.<sup>[19]</sup> The outer surface of the cucurbit[n]uril is composed of a large number of nitrogen atoms and carbon atoms and the cavity has a certain degree of hydrophobicity that can form a stable host-guest inclusion complex with a guest molecule via non-bonding interactions, such as hydrogen bonds, van der Waals forces and ionic dipoles.<sup>[20–27]</sup> It has been proved that cucurbit[n]urils can be used as non-toxic and safe drug carriers,<sup>[28–30]</sup> among which cucurbit[8]uril (Q[8])<sup>[31]</sup> has a large cavity with certain application value in increasing the solubility,<sup>[32]</sup> stability<sup>[33]</sup> and release rate<sup>[34]</sup> of drug molecules. However, research studies on using cucurbit[n]urils as a drug carrier for chloramphenicol have not been reported to date. Herein, Q[8] was selected as the host and the host-guest interaction between Q[8] and CPE was studied using single-crystal X-ray diffraction, UV-Vis and <sup>1</sup>H NMR spectroscopy, and the effects of Q[8] on the stability, in vitro release rate and antibacterial activity of CPE were investigated.

## Results and discussion

## 2.1 The host-guest interaction between Q[8] and CPE

### 2.1.1 Single-crystal structure analysis of CPE@Q[8]

The clathrate mode and crystal parameters of CPE and Q[8] were determined on Bruker D8 Venture single-crystal diffractometer and shown in Figure 2 and Table S1, respectively. Figure 2(A) shows the interaction of CPE and Q[8] results in an asymmetric CPE@Q[8] structure, including one Q[8] and one CPE molecule and the entire CPE molecule enters the Q[8] cavity. Therefore, Q[8] and CPE form a 1:1 host-guest inclusion complex (CPE@Q[8]). Figure 2(B) shows the O20 atom of the CPE molecule and the port oxygen atom (O5) of Q[8] interact through the formation of a O-H...O hydrogen bond, in which the bond distance between O20 and O5 was 2.921 Å. It can be seen that the CPE molecule is distorted at the C51 atom and the bond angle between C53-C51-N34 was 103.30°, which makes the CPE molecule fixed and enter the cavity of Q[8]. Figure 2C shows the crystal structure stacking diagram of the CPE@Q[8] host-guest complex along the c-axis. It can be clearly seen that small hexagonal holes are formed between the complexes, which are expected to have potential applications in molecular adsorption and drug delivery.

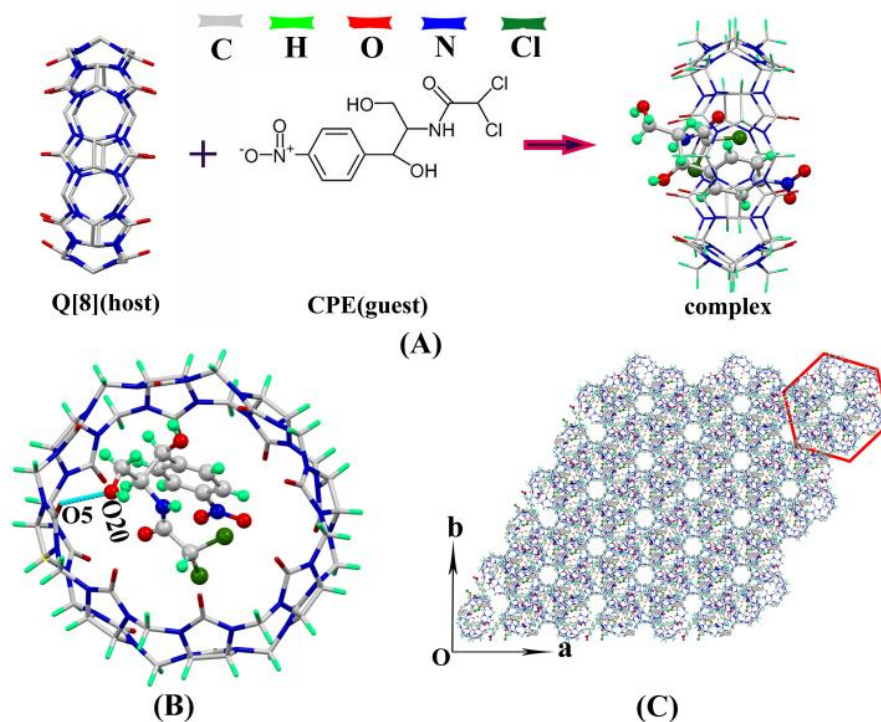


Fig.2 (A)CPE and Q[8] structural model diagram, (B) Interaction between CPE

and Q[8], (C) CPE@Q[8] Stacked graph along the c-axis

### 2.1.2 UV-Visible spectroscopy

The interaction between Q[8] and CPE was investigated using UV-Vis spectroscopy utilizing the molar ratio and Job's method under neutral conditions (Fig. 3). Fig. 3A shows that CPE has a strong absorption peak at  $\lambda = 278$  nm and the absorption intensity gradually decreases after the continuous addition of Q[8]. When  $n(\text{Q[8]}):n(\text{CPE}) = 1:1$ , the absorbance exhibits an obvious turning point and further increasing the concentration of Q[8] does not change the absorption of the system. The spectrogram determined using Job's method is shown in Figure 3(B). When  $n(\text{Q[8]})/[n(\text{Q[8]})+n(\text{CPE})] = 0.5$ , the maximum value of  $\Delta A$  appears, indicating the formation of a 1:1 host-guest inclusion complex.

Due to the poor solubility of Q[8], an acid solution was selected as the medium to grow a crystal of the CPE@Q[8] host-guest inclusion complex. When the interaction between CPE and Q[8] was investigated using  $^1\text{H}$  NMR spectroscopy, a deuterated hydrochloric acid solution ( $V_{\text{D}_2\text{O}}:V_{\text{H}_2\text{O}} = 3:2$ ) was used as the NMR solvent. Consequently, the interaction between Q[8] and CPE in hydrochloric acid solution was studied (Fig. 3C and D). The results show that the molar ratio of CPE and Q[8] was 1:1 under acidic conditions, which was the same as that observed under neutral aqueous conditions.

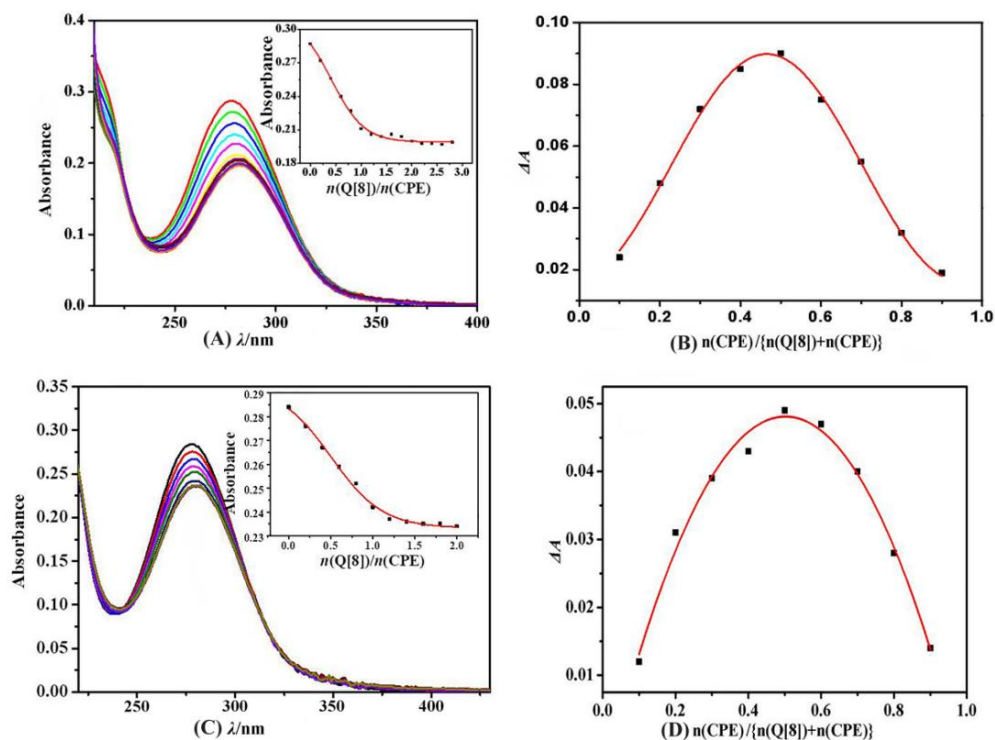


Fig.3 UV-Vis absorption spectra of CPE with Q[8] in aqueous solution (A) or hydrochloric acid solution (C) and UV-Vis Job's plot of  $\Delta A$  against  $n(\text{Q}[8]) / [n(\text{Q}[8]) + n(\text{CPE})]$  at 278 nm (B, D), ( $c_{(\text{CPE})} = 20 \mu\text{mol/L}$ )=a-o:0, 0.2, 0.4, 0.6, 0.8, 1.0, ..., 2.8)

### 2.1.3 ITC study of the interaction between CPE and Q[8]

ITC is a highly sensitive and automated microcalorimeter method, which can continuously and accurately monitor and record the calorimetric curve of each process to obtain the thermodynamic parameters and action ratio between the assemblies. Figure 4 and Table 1 show the exothermic isotherms and thermodynamic constants obtained for the titration of CPE with Q[8] interaction using ITC. From the data, it can be seen that the reaction was enthalpy driven and its binding constant was  $8.057 \times 10^5 \text{ L/mol}$ .

**Table 1** Thermodynamic parameters related to the CPE@Q[8] system at 25°C

Complex	$K/(\text{L}\cdot\text{mol}^{-1})$	$\Delta G/(\text{kJ}\cdot\text{mol}^{-1})$	$\Delta H/(\text{kJ}\cdot\text{mol}^{-1})$	$T\Delta S/(\text{kJ}\cdot\text{mol}^{-1})$
CPE@Q[8]	$8.057 \times 10^5$	-34.63	-43.53	11.66

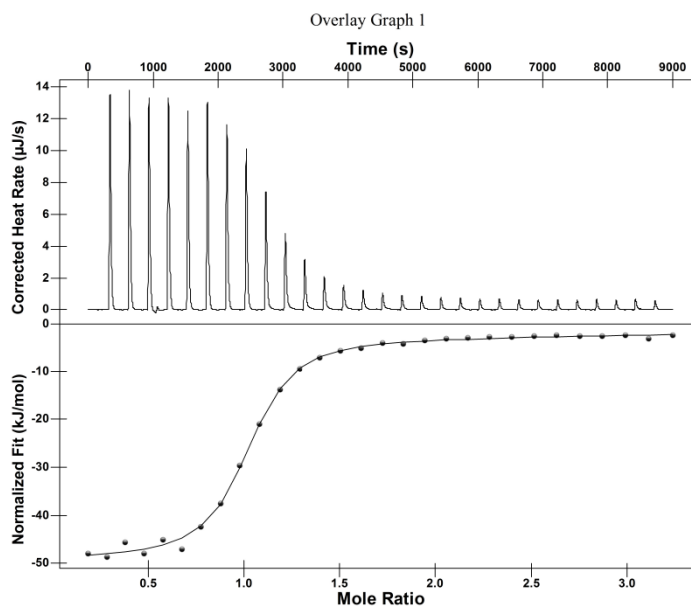


Fig. 4 ITC data obtained for the binding of Q[8] with CPE in an aqueous solution at 25 °C

#### 2.1.4 <sup>1</sup>H NMR spectroscopy

<sup>1</sup>H NMR spectroscopy is one of the most important methods used to explore the host-guest interaction mode. Through the interaction of the cucurbit[n]uril on the guest molecule, the chemical shift of the proton resonance peaks of the guest can be observed in water, so a mixed solution of deuterated hydrochloric acid and deuterated water was used as the NMR solvent. After adding Q[8], the chemical shifts of all proton resonance peaks of CPE are shifted toward the high field region, so it can be inferred that the whole CPE molecule enters the cavity of Q[8], which is consistent with our single-crystal X-ray analysis of CPE@Q[8] shown in Figure 2.

Table 2. Changes in <sup>1</sup>H NMR chemical shift of CPE after the addition of Q[8] (V<sub>D2O</sub>:V<sub>H2O</sub>=3:2) of Q[8]

<sup>1</sup> H nucleus	2-H、6-H	3-H、5-H	7-H	8-H	9-H	11-H
$\Delta\delta/\text{ppm}$	0.64	0.81	0.39	0.24	0.23	0.57

\*The formula for calculating the chemical shift of the proton resonance peak caused by the coordinated combination of CPE and Q[8] is as follow:  $\Delta\delta = \delta_{\text{complex}} - \delta_{\text{free}}$ .

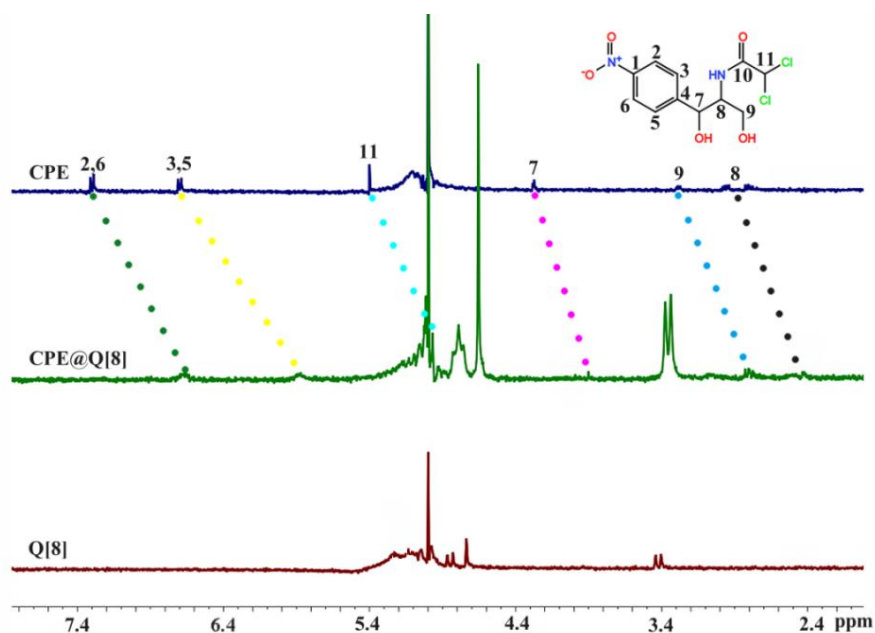


Fig. 5  $^1\text{H}$  NMR spectra of CPE, CPE@Q[8] and Q[8] ( $V_{\text{D}_2\text{O}}:V_{\text{H}_2\text{O}}=3:2$ )

### 2.1.5 IR spectroscopy

Fig. 6 shows the IR spectra recorded for Q[8] (a), CPE (b), a physical mixture of Q[8] and CPE  $\{n(\text{Q}[8])/n(\text{CPE}) = 1:1\}$  (c) and the CPE@Q[8] inclusion complex (d). By comparison, spectrum (c) is a simple superposition of the spectra recorded for Q[8] (a) and CPE (b), and there was no interaction. When comparing (c) and (d), the C-H stretching vibration peak was observed at  $3100\text{ cm}^{-1}$  and the C=C skeleton vibration peaks of the benzene ring of CPE were observed at  $1603$ ,  $1520$  and  $1413\text{ cm}^{-1}$ ; the bending vibration peaks of the O-H bonds were observed at  $1106$  and  $1066\text{ cm}^{-1}$ . The nitro-symmetric tensile vibration peak observed at  $1503\text{ cm}^{-1}$  and the nitro-asymmetric tensile vibration peak at  $1320\text{ cm}^{-1}$  disappeared in the spectrum (d). At the same time, the fingerprint region peak of the benzene ring observed from  $500$  to  $900\text{ cm}^{-1}$  disappeared or weakened. Therefore, it can be inferred that CPE interacts with Q[8].



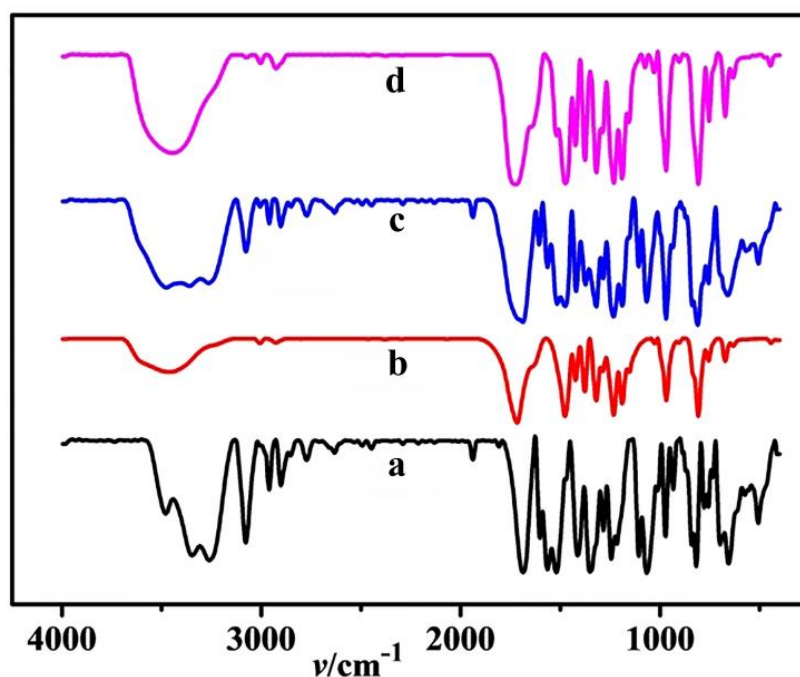


Fig.6 IR spectra recorded for Q[8](a), CPE(b), a physical mixture of Q[8] and CPE(c), and the CPE@Q[8] inclusion complex(d)

## 2.2 The effect of Q[8] on the properties of CPE

### 2.2.1 Stability analysis

The stability of CPE and CPE@Q[8] in artificial gastrointestinal juice was investigated using UV-Vis spectroscopy. Figure 7A shows the variation of the UV absorption intensity of CPE and CPE@Q[8] over time in simulated gastric juice (pH = 1.2). Figure 7B shows the relationship between the UV absorption intensity of CPE and its inclusion complex in artificial intestinal fluid (pH = 6.8) with time. The results show that CPE itself has high stability in artificial gastrointestinal juice and the intervention of Q[8] did not change its stability.

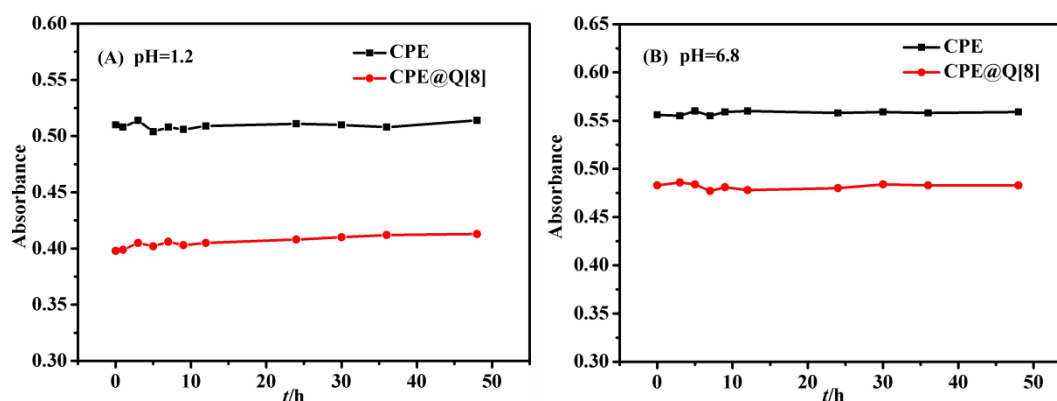


Fig. 7 the UV absorption intensity of CPE and CPE@Q[8] changes with time in

the artificial gastrointestinal juice (pH=1.2, pH=6.8)

## 2.2 Drug release behavior in vitro

Figure 8 shows the release curve obtained for CPE and its inclusion complex in artificial gastrointestinal juice. Figure 8A shows that CPE was completely released after ~1.3 h in artificial gastric juice (pH = 1.2) and its release rate was 88.19%. CPE@Q[8] basically reached a release equilibrium after 9 h and the cumulative release rate was 51.26%. It is possible that the inclusion of CPE in Q[8] causes its release rate to be reduced and has a slow-release effect. In artificial intestinal fluid, CPE reached the release end point after 1.67 h, and its in vitro cumulative release rate was 85.63% (Fig. 8B). The release rate of CPE@Q[8] was faster before 2 h, but the release rate was slow after 2 h, and its cumulative release rate was 32.59% after 12 h. The results show that the incorporation of CPE in Q[8] has a slow-release effect on the artificial gastrointestinal juice.

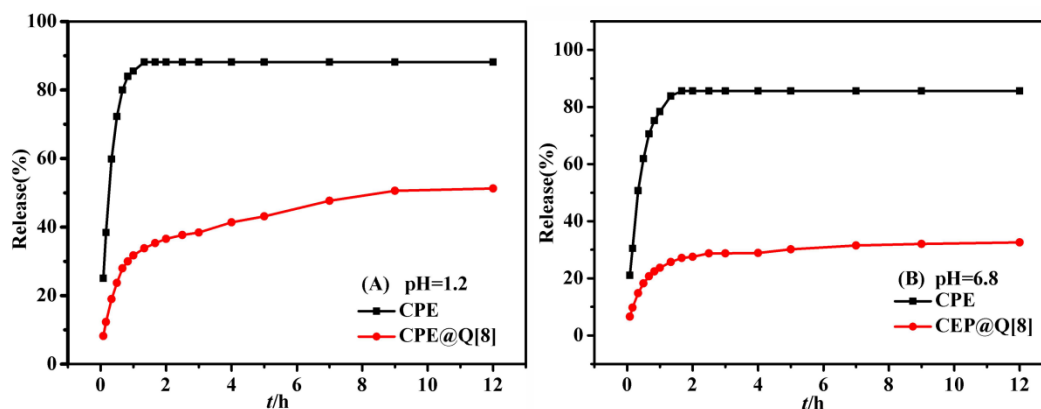


Fig.8 Release curve of CPE and CPE@Q[8]In artificial gastrointestinal juice (pH=1.2, pH=6.8)

## 2.3 Antibacterial activity

The minimum inhibitory concentration (MIC) of CPE and CPE@Q[8] was determined using the test tube double dilution method (Table 2). The results showed that the MIC of CPE and CPE@Q[8] against *E. coli* was  $1.5 \times 10^{-3}$  and  $1.0 \times 10^{-3}$  mol/L, respectively. The intervention of Q[8] increased the anti-*E. coli* effect of CPE by 1.5 times. The MIC values of CPE and CPE@Q[8] on *Staphylococcus aureus* (SA) were both  $2.0 \times 10^{-3}$  mol/L, and the intervention of Q[8] had no effect on CPE against SA.

Table 2 The minimum effective concentration (MIC) of CPE, CPE@Q[8] against Escherichia coli and S. aureus

Sample	MIC ( mol/L )	MIC ( mol/L )
	E.coli	SA
CPE	$1.5 \times 10^{-3}$	$2.0 \times 10^{-3}$
CPE@Q[8]	$1.0 \times 10^{-3}$	$2.0 \times 10^{-3}$

## Conclusions

Herein, the 1:1 host-guest complex of CPE and Q[8] was confirmed using single-crystal X-ray diffraction and  $^1\text{H}$  NMR, UV-Vis and IR spectroscopy. The CPE molecule completely enters the cavity of Q[8] with an inclusion constant of  $5.4736 \times 10^5 \text{ L/mol}$ . The intervention of Q[8] has no effect on the stability of CPE, which has a slow-release effect on CPE in artificial gastrointestinal juice and improves the inhibitory ability of CPE against *E. coli*. Our experimental results provide a theoretical basis for the application of CPE.

## Funding

The Science and Technology Support Plan of Guizhou Province (GuiZhou Science and Technology Cooperation Support (2020)4Y218) is acknowledged.

## References

- [1] Lewis, E. A.; Adamek, T. L.; Vining, L. C.; White, R. L. *J.Nat. Prod.* **2003**, 66, 62–66. doi: 10.1021/np020306e
- [2] Brooks, M. H.; Smith, R. L.; Macalady, D. L.; *Appl. Environ. Microb.* **1992**, 58, 1746–1753. doi:10.1128/aem.58.5.1746-1753.1992
- [3] Aiassaa, V.; Zoppi, A.; Albesa, I.; Longhi, M. R. *Carbohydr. Polym.* **2015**, 121, 320–327. doi:10.1016/j.carbpol.2014.11.017
- [4] Aiassa, V.; Zoppi, A.; Becerraa, M. C.; Albesa, I.; Longhi, M. R. *Carbohydr. Polym.* **2016**, 152, 672-678. doi:10.1016/j.carbpol.2016.07.013
- [5] Shi, J. H.; Zhou, Y. F. *Spectrochim. Acta A.* **2011**, 83, 570-574. doi:10.1016/j.saa.2011.09.005
- [6] Gannimani, R.; Ramesh, M.; Mtambo, S.; Pillay, K.; Soliman, M. E.; Govender,

- P. J. Inorg. Biochem.* **2016**, 157,15-24. doi:10.1016/j.jinorgbio.2016.01.008
- [7] Freeman, W. A.; Mock, W. L.; Shih, N. Y. *J. Am. Chem. Soc.* **1981**, 103, 7367-7368. doi:10.1021/ja00414a070
- [8] Kim, K.; Selvapalam, N.; Oh, D. H.; *J. Incl. Phenom. Macro.* **2004**, 50, 31-36. doi:10.1007/s10847-003-8835-7
- [9] Day, A.; Arnold, A. P.; Blanch, R. J.; Sunshall, B.; *J. Org. Chem.* **2001**, 66, 8094-8100. doi:10.1021/jo015897c
- [10] Day, A.; Blanch, R. J.; Arnold, A. P.; Lewis, G. R.; Lorenzo, S. *Angew. Chem.* **2002**, 41, 275-277. doi:10.1002/1521-3773(20020118)41:2%3C275::AID-ANIE275%3E3.0.CO;2-M
- [11] Liu, S.; Zavalij, P. Y.; Isaacs, L. *J. Am. Chem. Soc.* **2005**, 127, 16798-16799. doi:10
- [12] Cheng, X. J.; Liang, L. L.; Chen, K.; Ji, N. N.; Xiao, X.; Zhang, J. X.; Zhang, Y. Q. S.; Xue, F.; Zhu, Q. J.; Ni, X. L.; Tao, Z. *Angew. Chem. Int. Edit.* **2013**, 52, 7252-7255. doi:10.1002/ange.201210267.1021/ja056287n
- [13] Flinn, A.; Hough, G. C.; Stoddart, J. F.; Williams, D. J. *Angew. Chem. Int. Edit.* **1992**, 31, 1475-1477. doi:10.1002/anie.199214751
- [14] Wu, F.; Wu, L. H.; Xiao, X.; Zhang, Y. Q.; Xue, S. F.; Tao, Z.; Day, A. I. *J. Org. Chem.* **2012**, 77, 606-611. doi:10.1021/jo2021778
- [15] Wu, L. H.; Ni, X. L.; Wu, F.; Zhang, Y. Q.; Zhu, Q. J.; Xue, S. F.; Tao, Z. *J. Mol. Struct.* **2009**, 920, 183-188. doi:10.1016/j.molstruc.2008.10.057
- [16] Jon, S. Y.; Selvapalam, N.; Oh, D. H.; Kang, J. K.; Kim, S. Y.; Jeon, Y. J.; Lee, J. W.; Kim, K. *J. Am. Chem. Soc.* **2003**, 125, 10186-10187. doi:10.1021/ja036536c
- [17] Isobe, H.; Sato, S.; Nakamura, E.; *Org. Lett.* **2002**, 4, 1287-1289. doi:10.1021/ol025749o
- [18] Nau, W. M.; Florea, M.; Assaf, K. I. *Isr. J. Chem.* **2011**, 51, 559-577. doi:10.1002/ijch.201100044
- [19] Whitesides, G. M.; Simanek, E. E.; Mathias, J. P.; Seto, C. T.; Chin, D.; Mammen, M.; Gordon, D. M.; *Acc. Chem. Res.* **1995**, 28, 37-44. doi:10.1021/ar00049a006
- [20] Hunter, C. A.; J. K. M. Sanders, *J. Am. Chem. Soc.* 1990, 112, 5525-5534. doi:0002-7863/90/1512-5525\$02.50/0
- [21] Nishio, M.; Umezawa, Y.; Hirota, M.; akeuchi, Y. *Tetrahedron* **1995**, 51, 8665-8701. doi:10.1016/0040-4020(94)01066-9

- [22] Sun, J. P.; Guo, P. P.; Liu, M.; Li, H. *J. Mater. Chem. C* **2019**, *7*, 8992-8999. doi:10.1039/c9tc02666e
- [23] Shi, L. L.; Liu, M.; Li, H. *CrystEngComm* **2020**, *22*, 3753-3758. doi:10.1039/d0ce00603c
- [24] Ambler, J.; Brown, L.; Cockcroft, X. L.; Grütter, M.; Hayler, J.; Janus, D.; Jones, D.; Kane, P.; Menear, K.; Priestle, J.; Smith, G.; Talbot, M.; Walker, C. V.; Wathey, B. *Bioorg. Med. Chem. Lett.* **1999**, *9*, 1317-1322. doi:10.1016/S0960-894X(99)00172-9
- [25] Gui, X. Y.; Liu, C.; Li, F. Y.; Wang, J. F.; *Ecotoxicol. Environ. Saf.* **2020**, *197*, 110597. doi:10.1016/j.ecoenv.2020.110597
- [26] Axtmann, M.; Heier, M.; Hilali, W.; Weigand, B. *Int. J. Heat Mass Tran.* **2016**, *103*, 974-983. doi:10.1016/j.ijheatmasstransfer.2016.07.091
- [27] Heo, J.; Kim, S. Y.; Whang, D.; Kim, K. *Angew. Chem. Int. Edit.* **1999**, *38*, 641-643. doi:10.1002/(SICI)1521-3773(19990301)38:5%3C641::AID-ANIE641%3E3.0.CO;2-O
- [28] Buschmann, H. J.; Cleve, E.; Jansen, K.; Wego, A.; Schollmeyer, E. *J. incl. Phenom. Macro.* **2001**, *40*, 117-120. doi:10.1023/A:1011159119554
- [29] Zhao, Y. J.; Bali, M. S.; Cullinane, C.; Day, A. I.; Collins, J. G.; *Dalton T.* **2009**, *26*, 5190-5198. doi:10.1039/B905112K
- [30] Xu, Z. L.; Lian, X. W.; Li, M. J.; Zhang, X. D.; Wang, Y.; Tao, Z.; Zhang, Q. J. *Chem. Res. Chinese U.* **2017**, *33*, 736-741. doi:10.1007/s40242-017-7096-8
- [31] Xie, J.; Zeng, Z. S.; Tao, Z.; Zhang, Q. J. *Chem. Res. Chinese U.* **2020**, *36*, 804-809. doi: 10.1007/s40242-020-0005-6
- [32] Huang, J. J.; Xu, Z. L.; Lian, X. W.; Zhang, X. D.; Tao, Z.; Zhou, Q. D.; Zhang, Q. J.; Wei, G. *Chem. J. Chinese U.* **2018**, *39*, 2425-2432. doi: 10.7503/cjcu20180337
- [33] Zeng, Z. S.; Xie, J.; Luo, G. Y.; Tao, Z.; Zhang, Q. J. *Beilstein J. Org. Chem.* **2020**, *16*, 2332-2337. doi:10.3762/bjoc.16.194
- [34] Zhang, X. D.; Xie, J.; Xu, Z. L.; Tao, Z.; Zhang, Q. J. *Beilstein J. Org. Chem.* **2020**, *16*, 71-77. doi:10.3762/bjoc.16.9